PNAS
www.pnas.org

Supplementary Information for

Oscillations in the central brain of *Drosophila* are phase locked to attended visual features

Martyna J. Grabowska, Rhiannon Jeans, James Steeves, & Bruno van Swinderen

Bruno van Swinderen
Email: bvanswinderen@uq.edu.au

This PDF file includes:

Supplementary text
Figures S1 to S12
Supplementary References

www.pnas.org/cgi/doi/10.1073/pnas.2010749117

Supplementary Information Text

Supplementary Methods

Preparation.

Animals were immobilized under cold anesthesia (0.5°C) for 60s and positioned for tethering on a custom-made preparation block. The flies were then glued dorsally to a tungsten rod by means of dental cement (Coltene Whaledent Synergy D6 Flow A3.5/B3) and cured with blue light (Radii Plus, Henry Schein Dental). To avoid movement artefacts due to wing movements of the fly, its wings were folded up and glued to the tungsten rod with dental cement. The head was immobilized by gluing it to the thorax with dental cement. After tethering, the animals were provided with water and allowed to rest for about 30 min before further preparation and testing. To access the brain for recordings, a small rectangular-shaped portion of the cuticle around the ocelli was cut out with a 0.3mmx13mm syringe (BD Microlance) and the edges of the rectangle were surrounded by dental cement in order to form a walled pod around the open brain section. The pod was filled with oxygenated extracellular solution (in mM): 103 NaCl, 10.5 trehalose, 10 glucose, 26 NaHCO3, 5 C6H15NO6S, 5 MgCl2 (hexa-hydrate), 2 sucrose, 3 KCl, 1.5 CaCl (dihydrate), and 1 NaH2PO4, which was regularly renewed during the experiment in order to ensure sufficient oxygenation of the fly brain. To facilitate access to the brain and dissolve non-neuronal tissue, 0.5% collagenase/extracellular solution was applied directly in the fly head and flushed out with pure extracellular solution after 20s.

Electrophysiological Analysis.

Using MATLAB 2019, all local field potential (LFP) data were first downsampled to 1000Hz. To analyze the LFP data in the time-frequency domain we applied a Morlet wavelet transformation using a custom written MATLAB script and the Fieldtrip toolbox (1). We used a 0.01Hz spectral resolution and a 30ms time window sliding every 5ms in the open-loop experiments, and a 0.01Hz spectral resolution and a 20ms time window sliding every 7ms in the closed-loop experiments. To average the closed-loop data, we first extracted the average LFP power for both input frequencies (5.9Hz±0.2Hz and 6.6Hz±0.2Hz), when either the small bar or the larger bar was in the frontal visual field (FVF), or in the periphery, for each condition. For this purpose, we binned all LFP data according to positions of the stimuli on our 6 LED panels (60° wide each) and averaged all instances when a bar was on a specific panel. For all experiments, we defined the first 5s prior to stimulus presentation in open loop and closed loop as baseline. For baseline normalization we used the time domain averaged Morlet wavelet coefficient amplitude for each extracted frequency domain during baseline. We then divided the Morlet wavelet coefficient amplitude during stimulation for both input frequencies separately by the baseline average. We first normalized data from each animal, then averaged all trials corresponding to every condition for each animal, before averaging across animals. In some cases, we normalized the data between [0 1] in order to compare differences in range between conditions.

For the analysis of LFP power after visual perturbations, we extracted all instances of perturbations and partitioned the data for when the small or the large bar were in the FVF. We used epochs of 500ms pre-perturbation (baseline) and 2s post-perturbation, and subsequently ran a time-frequency analysis for each epoch. We subtracted the averaged LPF power during baseline from the post-perturbation LFP power, averaged this for each animal, and then averaged across animals. Finally, we z-scored the spectrogram data and plotted the significant changes from baseline, which was set to 0. We performed the analysis for the stimulation frequencies as well as 10-20Hz, 20-30Hz, 30-40Hz, 40-50Hz, and 50-100Hz.

Signal to noise ratio (SNR) of the frequency tags as well as z-scores were analyzed with Letswave6 (http://nocions.webnode.com/letswave) running on Matlab2016b. All LFP data were downsampled to 1000Hz, band-pass filtered between 0.1Hz-100Hz using a 4th order butterworth filter. For the open-loop experiments, every trial was segmented into 16s segments (20s stimulation, minus 2s after the start and 2s before the end of stimulation). We averaged these trials for each condition in the time domain separately for each animal. We then applied a fast

Fourier transformation to the averaged segments to reveal the tagged frequencies and harmonics. The SNR was calculated to exclude variable noise effects across animals and trials. The SNR was the ratio between the amplitude at the fundamental input frequencies of 5.9Hz and 6.7Hz and their surrounding frequency bins (20 bins, 10 on each side, excluding the immediately adjacent bin). Finally, we z-scored the data using the z-score function of Letswave6 to detect significances in frequency tags. For the analysis of endogenous oscillations we first applied a single frequency filter (for both input frequencies 5.9Hz and 6.6Hz and up to their 4th harmonic) with a range of ±0.1Hz around the peak frequencies using the iirnotch.m function of the MATLAB signal processing toolbox, to exclude the influence of our stimulation frequencies. We further removed line noise around 50Hz with the same function. Subsequently, we calculated the data in the time-frequency domain using Morlet Wavelet Transformation as described above for 10-20Hz, 20-30Hz, 30-40Hz, 40-50Hz and 50-100Hz, averaged the data over the period of visual stimulation, and performed a baseline subtraction of the average of the 5 s baselines for each trial. We averaged the power of each trial for each animal and then averaged the mean power across all animals.

The envelope-to-signal correlation (ESC) determines the correlation between the amplitude envelope of a filtered high frequency signal (in our case 20-30Hz and 30-40Hz) and the phase of the filtered low frequency signal (in our case our frequency tags 5.9Hz and 6.6Hz)(3) (Supplementary Figure 7). ESCs were performed using the MATLAB Toolbox Phase Amplitude Coupling Toolbox (4) for MATLAB. For this purpose, we first filtered the data for the corresponding frequency domains that are supposed to show the amplitude modulation (e.g 0.2-100Hz, Supplementary Figure 8; 20-50 Hz Figure 6) and the frequency domains that contained the stimulation frequencies (4-10Hz). We used the find_pac_shf.m function to calculate the ESC. This function compares the two signals by using the envelope amplitudes of the higher frequency bins and the phase of the lower frequency bins (phase calculated by using a Hilbert transformation for the frequency bins of the filtered data). To test for significance, the data were shuffled 200 times and, by applying a Pearson's correlation, significant positive correlations were extracted and plotted in a co-modulation map (Supplementary Figure 7, upper panels). ESCs were first calculated for every condition and then averaged to plot baseline vs stimulation activity. To compare ESC values between baseline and visual stimulation we extracted ESC values for the frequency bands for 20-30Hz and 30-50Hz and compared these between the conditions.
For open-loop conditions, phase locking values were calculated by extracting data phase locked to the stimulus onset (start of visual stimulation) and using 5s post-stimulus onset. 5s pre-stimulus onset was used for baseline conditions. Phase locking value (PLV) was calculated by applying a Hilbert transformation on the filtered data (5.9Hz±0.2Hz, 6.6±0.2Hz, 20-30Hz) and then applying the PLV.m function of the Phase-Locking-Value (5) toolbox for MATLAB (Eden M. Gerber (2020). PLV - phase locking value (https://www.mathworks.com/matlabcentral/fileexchange/71739-plv-phase-locking-value), MATLAB Central File Exchange. Retrieved January 8, 2020.). Baseline subtracted PLV values for each animal where bootstrapped using the MATLAB function bootstrap.m to create 1000 means and 95% confidence intervals (CI) were calculated using the function bootci.m. For closed-loop conditions, PLV was calculated on data extracted from successful fixations following a perturbation of the small and the large bar (stimulus was returned into FVF in less than 10s). We used epochs of 2s post-perturbation. 500ms pre-perturbation onset was used as baseline. Statistics was performed as for the open-loop condition.

Generation of simulated data for ESC analysis.

In order to test whether the significant increase in ESC and the PLV that we observed during dNPF circuit activation could be simply due to an increase in LFP amplitude for one of the frequency tags, we generated artificial data (Supplementary Figure 12) in which we kept the phase of our signals constant while manipulating the amplitude of select oscillations. For this purpose, we generated signals comprising both our stimulation frequencies (5.9Hz and 6.6 Hz) as well as two endogenous frequency domains (25-28Hz and 35-38Hz) and added Gaussian white

noise (WN) with a standard deviation of 2. For baseline conditions we used the same amplitudes for all frequencies. To simulate our data we used following equation:

$$sigBL = \sum_{k=25}^{n=28} \sin(2\pi * kt) + \sum_{k=35}^{n=38} \sin(2\pi * kt) + \sin(2\pi * 5.9t) + \sin(2\pi * 6.6t) + 2 * WN$$

In this equation, t is the time of our simulation, which was 10s at a sampling rate of 1000Hz. And WN is Gaussian white noise (Matlab command: WN=sigBL+randn(size(t))) added to the signal. We created a signal of 20s length where the first 10s described baseline (BL) and the next 10s post stimulus (stimulus onset was at 10s).

Signals generated post stimulus onset had different standard deviations in order to reproduce the differences in amplitudes observed in our data (See Supplementary Figure 12). We applied a fast Fourier Transformation on the simulated data, to confirm our frequency components. We then ran a ESC analysis as described above for our collected data to identify any significant correlations between our endogenous frequencies post stimulation and the stimulation frequencies. Simulation results were plotted the same way as for real data.

Frequency sweep

Canton-S fruit flies (3-10 days post-eclosion; 18 total) were put under cold anesthesia and tethered as described above. A sharpened fine tungsten wire (0.01-inch diameter, A-M Systems) acted as the reference electrode and was placed superficially into the thorax. Linear silicon probes with 16 electrode sites (Neuronexus Technologies) were inserted laterally into the eye of the fly and perpendicularly to the eye's curvature. Insertion was performed with the aid of a micromanipulator (Merzhauser), with the electrode recording sites facing posteriorly. For all experiments, probes had an electrode site separation of 25µm. This probe (375µm length) covered approximately half of the fly brain. Recordings were made using a multichannel data acquisition system with a sampling rate of 25kHz (Tucker-Davis Technologies). The probe was fully inserted until all electrode sites were in the fly head, which was confirmed by a significant reduction in 50Hz noise. This half-brain multichannel preparation has been described previously (8).The flickering stimuli were presented 5 times for each of the 10 flicker frequencies. The stimulus was active for 20s and the inter-trial interval was 2s. The stimulus order was randomly generated with MATLAB (MathWorks). As it has been demonstrated previously that ipsilateral stimuli produce the strongest lateral response in *Drosophila*, we decided to present the stimuli only on the ipsilateral LED panel. Data were downsampled to 1000Hz and high-pass filtered at 0.5Hz and low pass filtered at 200Hz using a Butterworth filter that caused zero phase distortion (filtfilt function, MATLAB). Line noise was reduced at 50Hz with the rmlinesmovingwinc.m function in the Chronux toolbox (9), using a window of 2s duration, and a step size of 1s. The data were bipolar referenced to create 15 functional channels. A multi-tapered Fourier transform was performed using the mtspectrumc.m Chronux function. Once in the frequency domain, data were baseline corrected by subtracting a 20s pre-stimulus period. For data analysis, we used central channels (channels 5-1), and the medians were taken over the channel and fly. The data were then imported into R (version 3.5.3) for statistical analysis. The R packages used included: lme4, influence.ME, nlme, ggplot2 (ggplot2 - Elegant Graphics for Data Analysis | Hadley Wickham | Springer), and their dependencies. Normality was tested by visually inspecting residuals and Q-Q-plots using the lmer function (lme4 R package). No skew or heteroscedasticity of variance was detected (11). Values that might skew a statistical analysis were detected using the influence.ME package (cooks.distance function) and variables higher than 4 times the mean cook's distance were replaced with the median (12) (total of 42 of 900 values). A linear mixed-effects model testing the sole influence of the frequency on the LFP power (LFP power ~ Stimulus Frequency + (1|Fly)) was then conducted using the restricted maximum likelihood method (REML) with the intercept set to 7.7Hz (nlme package) and 95% confidence intervals fit with the intervals function (Supplementary Figure 3A).

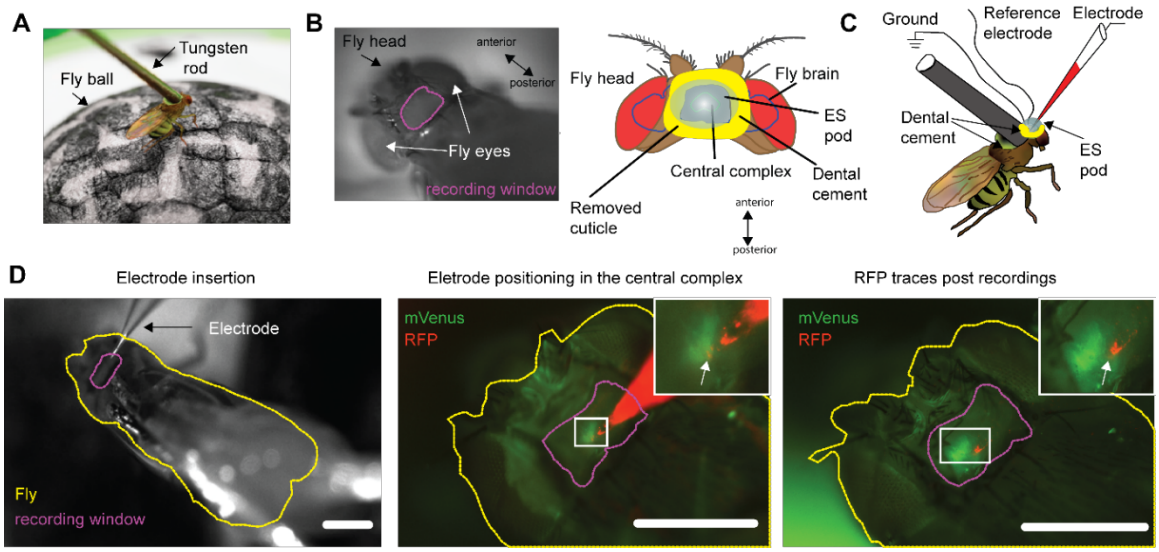

Fig. S1. mVenus-guided LFP recordings.

A) Fly placed on an air-supported ball, tethered to a tungsten rod. B) A close-up of the prepared fly head (left) and a schema of the recording preparation (right). Removal of the cuticle from the top of fly's head provides access to the central complex. ES=extracellular solution. C) Reference electrode and ground electrode were placed in the ES pod on the top of the fly head. D) Electrode insertion (left) guided by green-tagged fan-shaped body in dNPF-Gal4/ UAS-CsChrimson::mVenus flies. Red fluorescent protein (RFP) visible in the electrode was also used for guidance (middle). After recording (right) the electrode recording site is visible based on RFP released in proximity of the green fan-shaped body (box, arrow). Scale bar= 0.5mm.

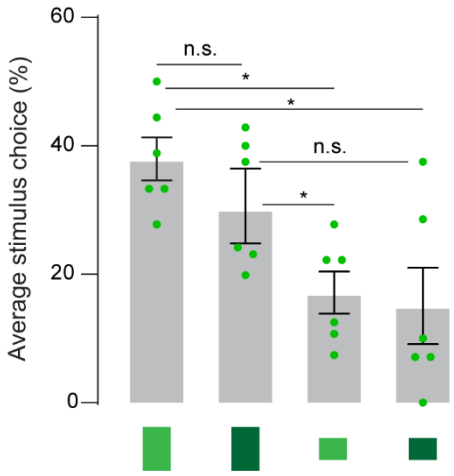

Fig. S2. Behavioral choices separated by stimulus brightness.

Stimulus choice averaged for all trials and experimental animals separated by stimulus brightness. (F(DFn,dFd)=4.852(3,20), p=0.0.107). One-way ANOVA with Tukey's multiple comparisons test, alpha=0.05. N=6, n=40. *p<0.05, n.s.=not significant.

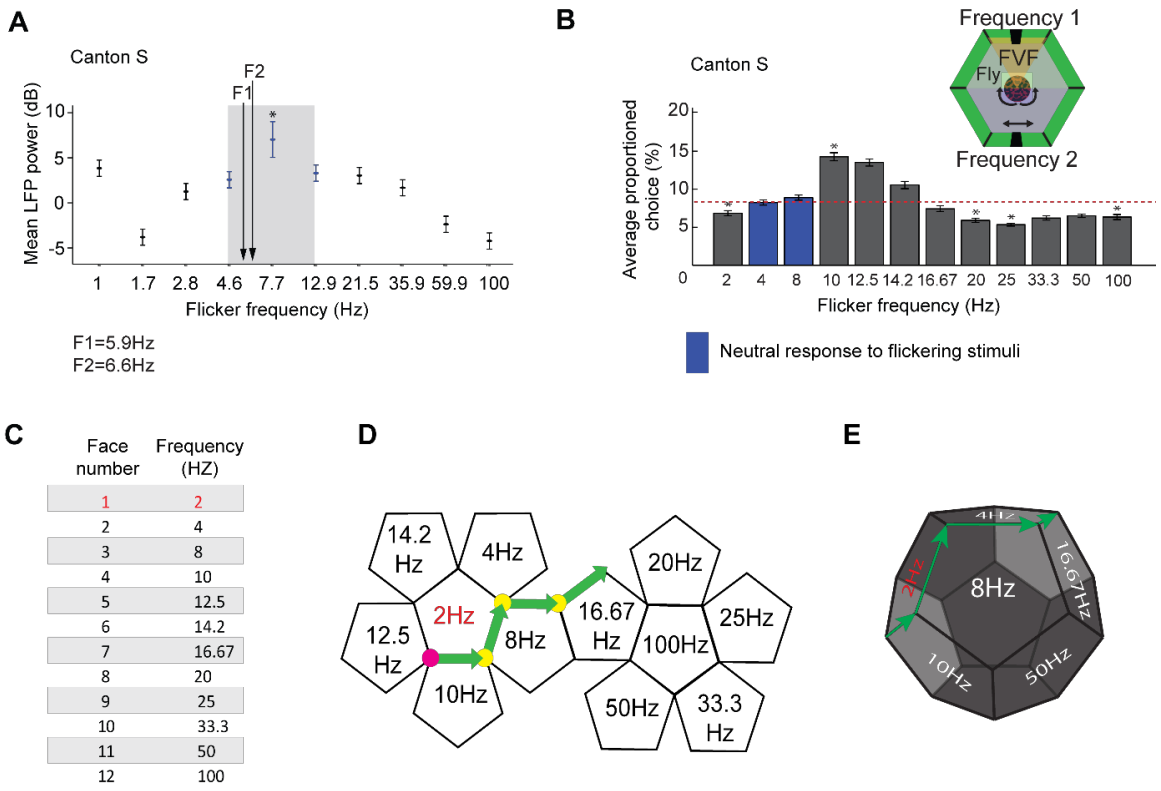

Fig. S3. Flicker frequency preferences and neural gain in LFP recordings.

A) Mean local field potential (LFP) power (dB) for 10 different flicker frequencies (see Methods). Canton S female flies, N=18; blue shading shows range evoking strongest neural response to visual flicker. Data shows estimated means with 95% confidence intervals. (Asterisk shown above 7.7Hz with a power value of 7.04 with a confidence interval 5.31- 9.11; the bounds do not overlap the confidence intervals of other frequencies). Arrows indicate flicker frequencies F1 and F2 chosen in this study. B) Average proportioned choice (%) for 12 different flicker frequencies in a multiple-choice paradigm (10). Female Canton S flies, N=24, Wilcoxon rank-sum test, $\alpha=0.05$, compared to 8.333% (random choice, red dotted line), error bars=SEMs. Blue=neutral visual flicker that do not evoke strong attraction or aversion. C) Table with all presented frequencies, each corresponding to one side of a geometric maze (D). Order of frequency combinations was defined by virtual path along edges of the virtual maze (E), green line, see Methods). *$p<0.05$, n.s.=not significant.

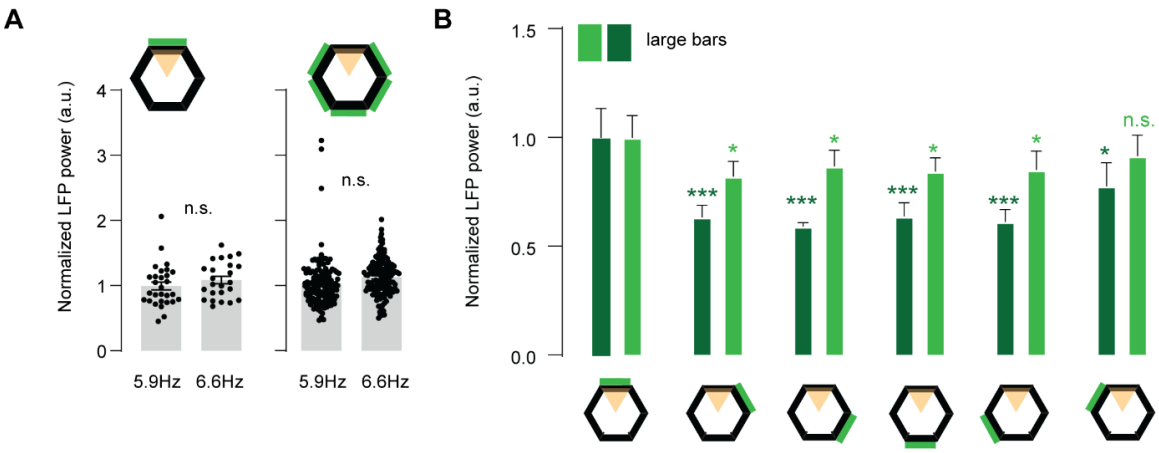

Fig. S4. LFP gain to different stimulus flicker frequencies and brightness depending on object position within LED arena.

A) Normalized local field potential (LFP) power for both stimulus frequencies in closed loop when stimulus was in the frontal visual field (FVF, yellow triangle) (left) and in every other position in the arena except the FVF (right). Data were analyzed by paired t-test on averaged LFP power for corresponding stimulus positions of each animal. Data points represent individual instances of averaged LFP power for the corresponding stimulus within the highlighted positions in the LED arena. B) LFP power normalized to the maximum LFP power of each brightness for the large bar. Statistical comparisons are between the mean normalized LFP power of the FVF to the rest of the arena for each contrast separately using a Kruskal-Wallis test. For both panels: N=6, error bars=SEM, dNPF-Gal4; UAS-CSChrimson(x)::mVenus flies, ATR-, *p<0.05 **p<0.01, p***<0.001, n.s.=not significant.

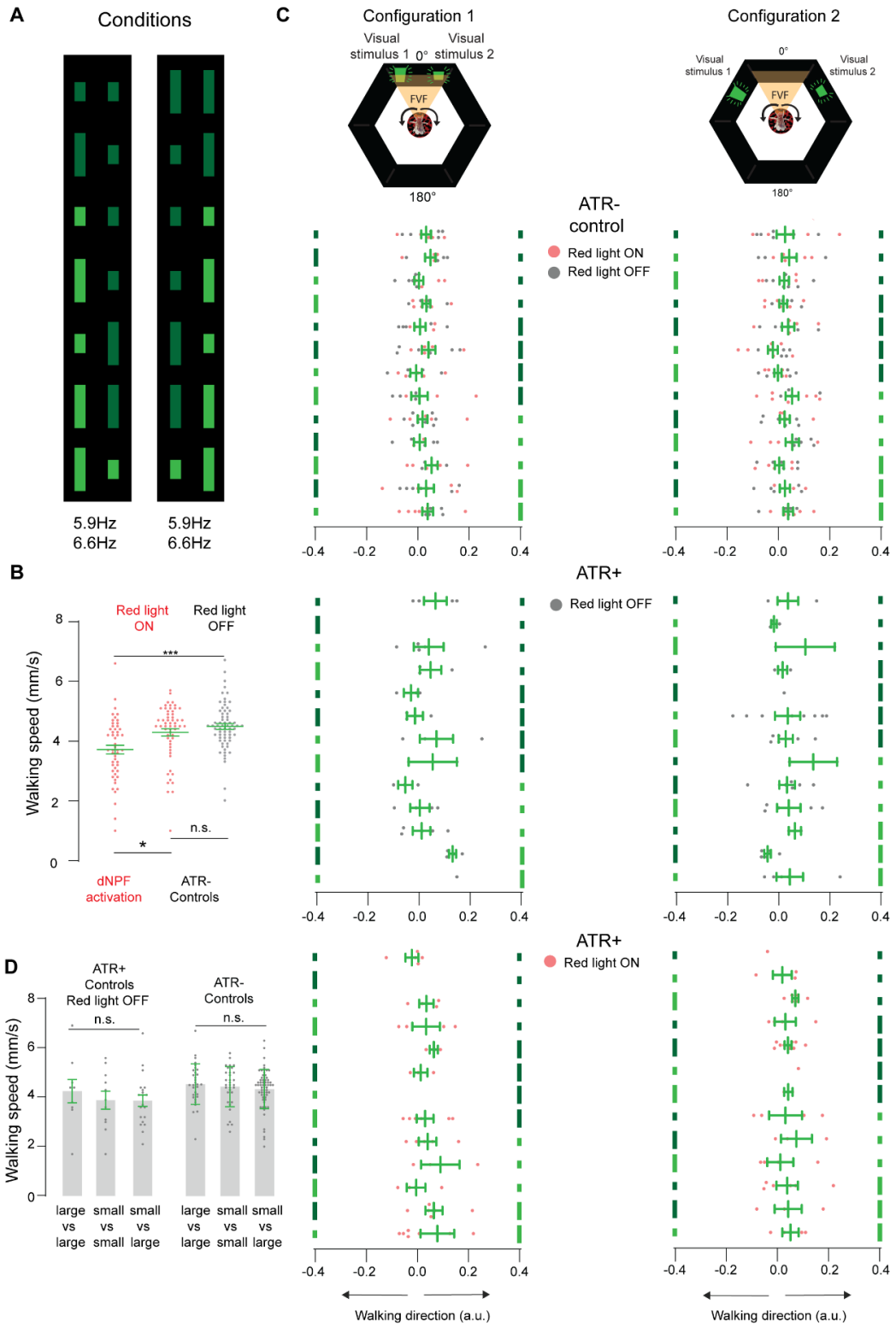

Fig. S5. Flies do not display walking direction preferences in the open-loop paradigm.

A) Flies were presented with 14 different conditions of paired visual stimuli. Stimuli differed in size, brightness, arena position, and flicker frequency. B) Mean walking speed during dNPF

activation. Each data point represents the average speed for all animals for a particular condition seen in (competing stimuli in A). Red represents conditions where red LEDs were turned on. dNPF activation represents animals fed with ATR and exposed to red light. ATR- represents control flies that have not been fed with ATR (see Methods). One-way ANOVA (F(DFn,dFd)=6.857(3,210), p=0.0002). C) Walking direction of the fly, extracted from turning direction of the ball. Arena schemas represent the two configurations for the stimulus position, narrow (configuration 1) and wide (configuration2). Data is shown for control (-ATR) and stimulation conditions (+ATR, with and without red light activation). Symbols on the left and right represent the stimulus pair for each condition in each configuration. Positive values represent a walking direction to the right side (the stimulus displayed on the right side) and negative values represent a walking direction to the left side (the stimulus displayed on the left side). Red data points show trials with red LEDs turned on, grey data points show trials with no red light. ANOVA Statistics for panels: Controls: Configuration 1 (F(DFn,dFd)=0.6642(12,119), p=0.78), configuration 2 (F(DFn,dFd)=1.024(12,126), p=0.43); ATR+ red LED OFF: Configuration 1 (F(DFn,dFd)=1.27(11,29), p=0.28), configuration 2 (F(DFn,dFd)=0.65(12,40), p=0.78), ATR+ red LED ON: Configuration 1 (F(DFn,dFd)=0.48(10,40), p=0.889), Configuration 2 (F(DFn,dFd)=0.29(12,39), p=0.98). D) Mean walking speed for all conditions, averaged across flies pooled for large vs large, small vs small and small vs large conditions for both configurations (F(DFn,dFd)=1.948(5,161),p=0.089). All data were compared with one-way ANOVA and a Tukey's multiple comparisons test, alpha=0.05. N=13 for controls (-ATR) and N=10 for ATR+. All data shows mean with SEM. n.s.=not significant, *p<0.05, ***p<0.001.

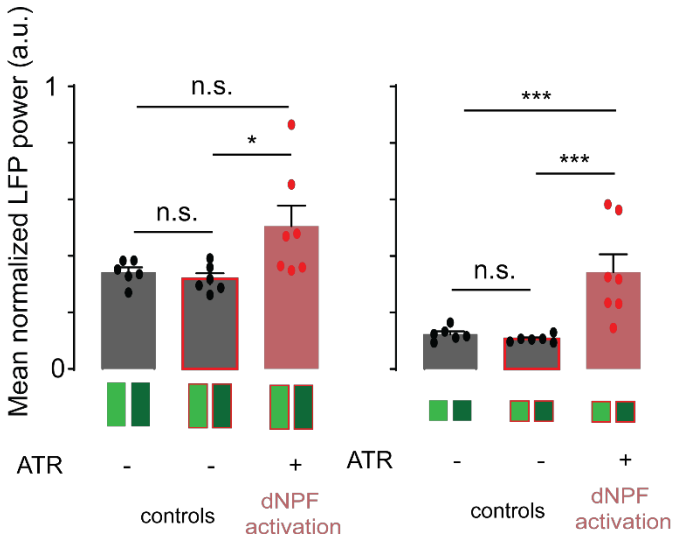

Fig. S6. dNPF circuit activation increases the gain for frequency tags associated with both visual objects.

Mean normalized LFP power for large bar (left) and small bar (right) for 2 controls (ATR-, no red LED light and ATR-, red LED light, N=6) and dNPF activation (ATR+, red LED light, N=7). Small object (right): ANOVA p=0.0012, F(DFn,dFd)=6.157(2,16); large object (left): ANOVA p=0.0267, F(DFn,dFd)=3.017(2,16), Tukey's multiple comparison test, α=0.05, error bars=SEM, n.s.=not significant, *p<0.05, ***p<0.001.

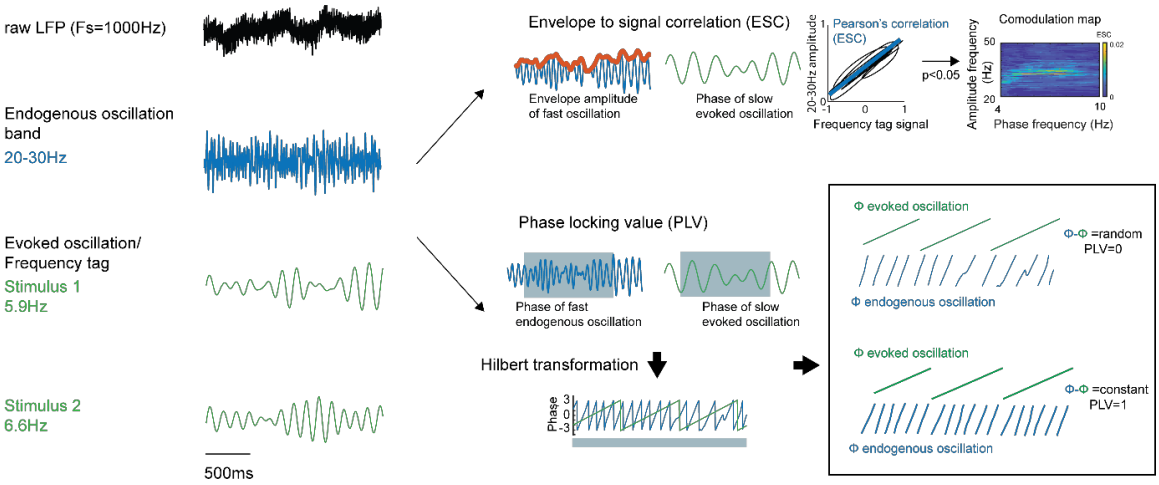

Fig. S7. Schemas showing analyses of phase amplitude coupling and phase locking.

Raw LFP data is first downsampled to 1000Hz and filtered for endogenous oscillation bands (blue, 20-30Hz in this example) and evoked oscillation frequency bands (green, stimulus 1 and stimulus 2, see Supplementary Methods). Envelope-to-signal correlation (ESC) (upper panels) is then calculated separately between the envelope amplitude of the endogenous oscillation bands (fast oscillation) and the phase of the slower, evoked oscillations. The phase (Φ) of the slower oscillations is calculated using a Hilbert transformation. The envelope signal and the phase values are then tested for significant correlations using the Pearson's correlation. Data that passes a threshold of $p<0.05$ is then plotted in a comodulation map. The phase locking value (PLV) (lower panels) is calculated by first applying a Hilbert transformation on each of the filtered data to define the instantaneous phase of the signal, and then calculating the difference between these phases over time. PLV covers a range between 0 (zero phase synchrony, or random) and 1, representing identical signals (constant).

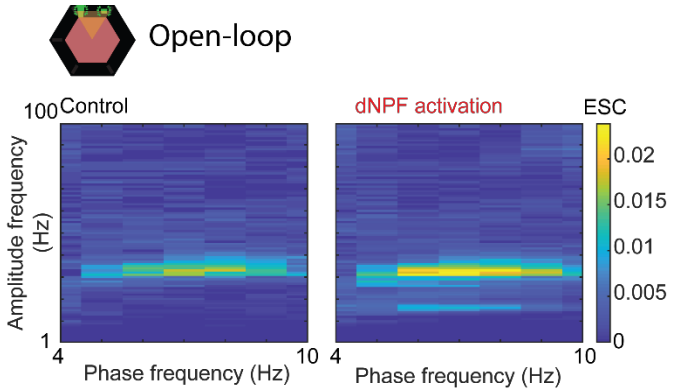

Fig. S8. Analysis of phase amplitude coupling.

Mean envelope to signal correlation (ESC) reveals a correlation between 20-50Hz and 4-10Hz during dNPF-circuit activation in open loop. Graphs show comodulation maps plotting ESC values with a Pearson's correlation above $p<0.05$. Control: ATR-, red LED light, N=6 dNPF activation=ATR+, no red LED light, N=7.

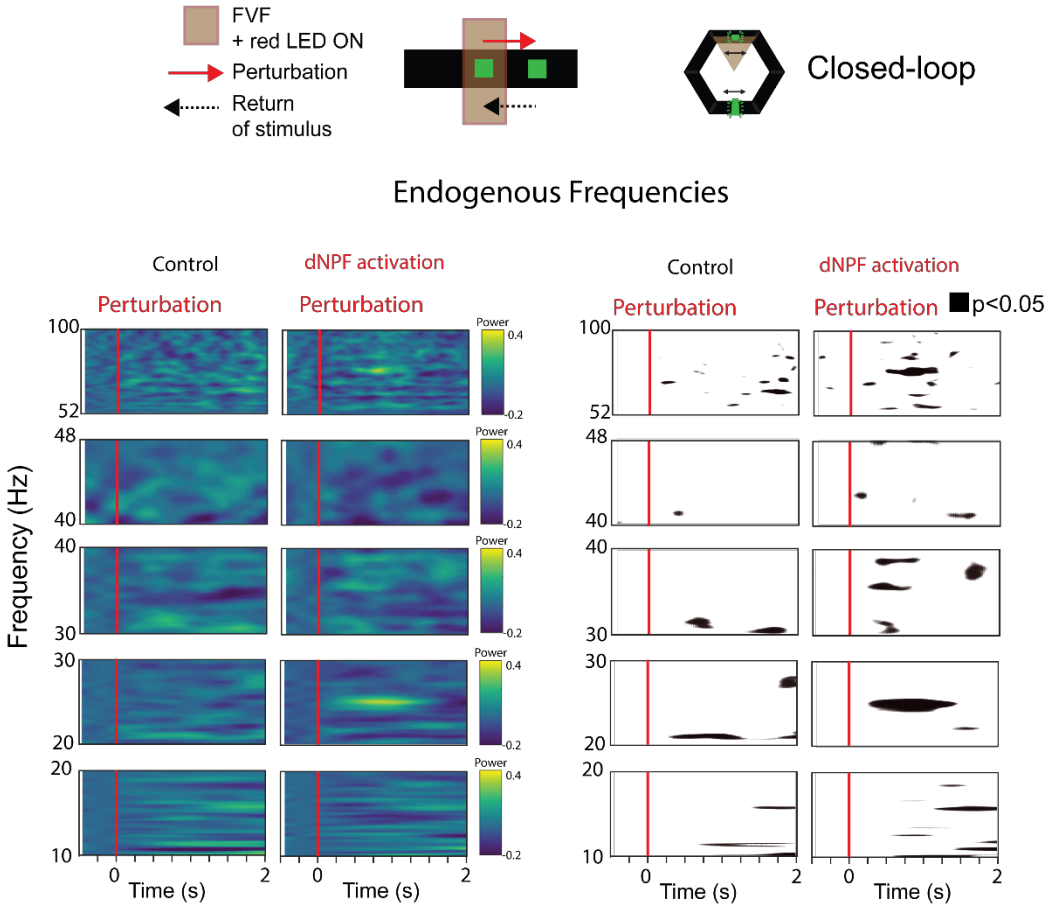

Fig. S9. Broad spectral responses (10-100Hz) following a perturbation of the small bar.

Top: Flies returning the small bar to the frontal visual field (FVF) activates dNPF circuit in closed-loop experiments. Bottom: colored spectrograms on the left show mean local field potential (LFP) power over time for all perturbations of a small bar for controls (ATR-, red LED light, left, N=6) and dNPF-circuit activation (ATR+, red LED light, right, N=9). Black and white spectrograms on the right show significant changes ($p<0.05$) of baseline corrected LFP power between baseline and post perturbation LFP power (z-scored data). Except for the 20-30Hz frequency domain (also shown in Figure 6E) there was no area of broad change of significant difference in LFP power for any frequency band between pre-perturbation baseline and post perturbation LFP activity between controls and dNPF activation.

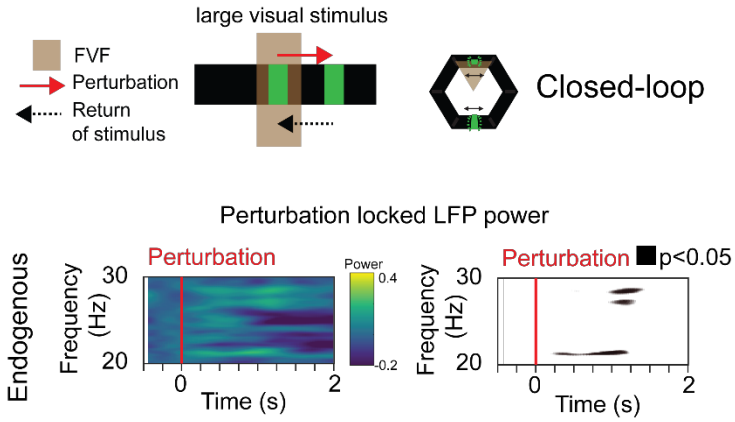

Fig. S10. Endogenous 20-30Hz responses following a perturbation of the large bar.

Top: Flies return the large bar to the frontal visual field (FVF) in closed loop, without activating dNPF circuits. Bottom left: Spectrogram showing mean LFP power after perturbation (red) normalized to local field potential (LFP) power 250ms pre perturbation. Bottom right: Statistically different values ($p<0.05$) from spectrogram plot on the left (z-scored data). ATR+, no red LED light, N=9.

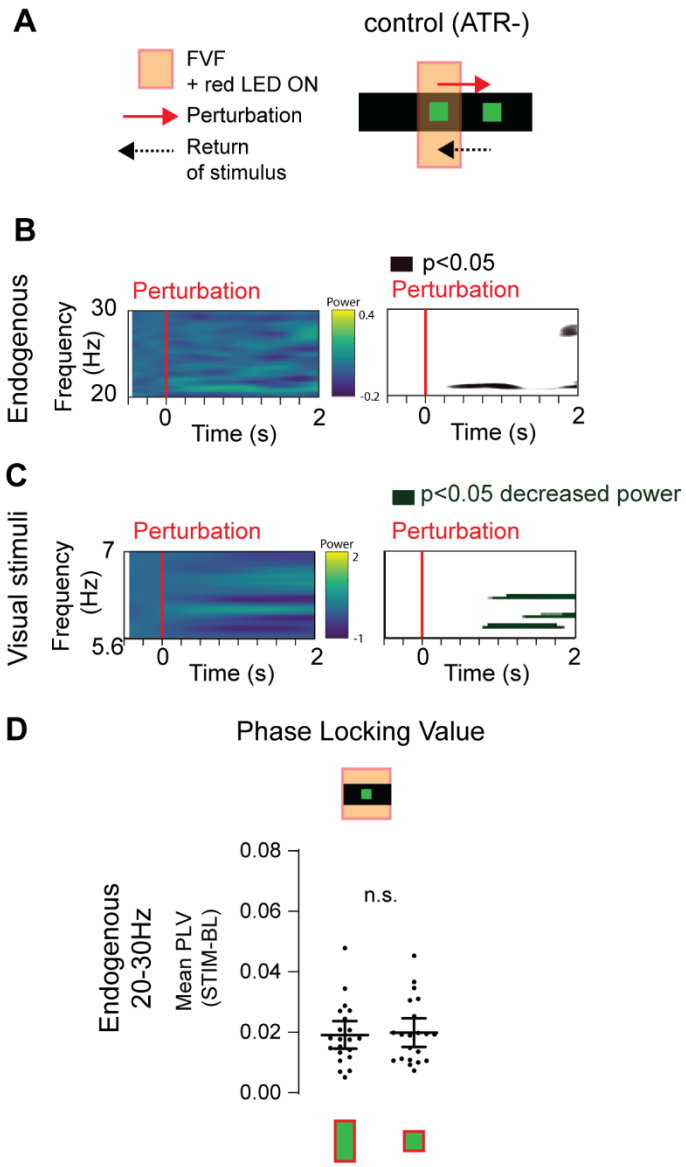

Fig. S11. Return of the small bar without dNPF-circuit activation does not result in increased phase locking between 20-30Hz and frequency tags associated with the small bar.

A) Control condition (ATR-, red LED light) for fixation behavior after perturbation for the small visual object. B) Left: Spectrogram showing mean LFP power over time for endogenous 20-30Hz frequency band. Right=spectrogram showing p-values significantly different ($p<0.05$) from pre perturbation baseline (z-scored data). (ATR-, red LED light, N=6). C) Left: Spectrogram showing mean LFP power over time for evoked frequencies during visual stimulation by small visual object. Right: Spectrogram showing p-values significantly different ($p<0.05$) from pre perturbation baseline (z-scored data). Note that this spectrogram shows a significant decrease in power between stimulus frequencies. (ATR-, red LED light, N=6). D) Mean PLV of evoked frequencies of visual objects and endogenous 20-30Hz oscillations. Baseline PLV values were subtracted from values during visual stimulation. (ATR-, red LED light, N=6 n=21 (bootstrapped data, mean with 95% confidence intervals, $p=0.8$, effect size=0.07).

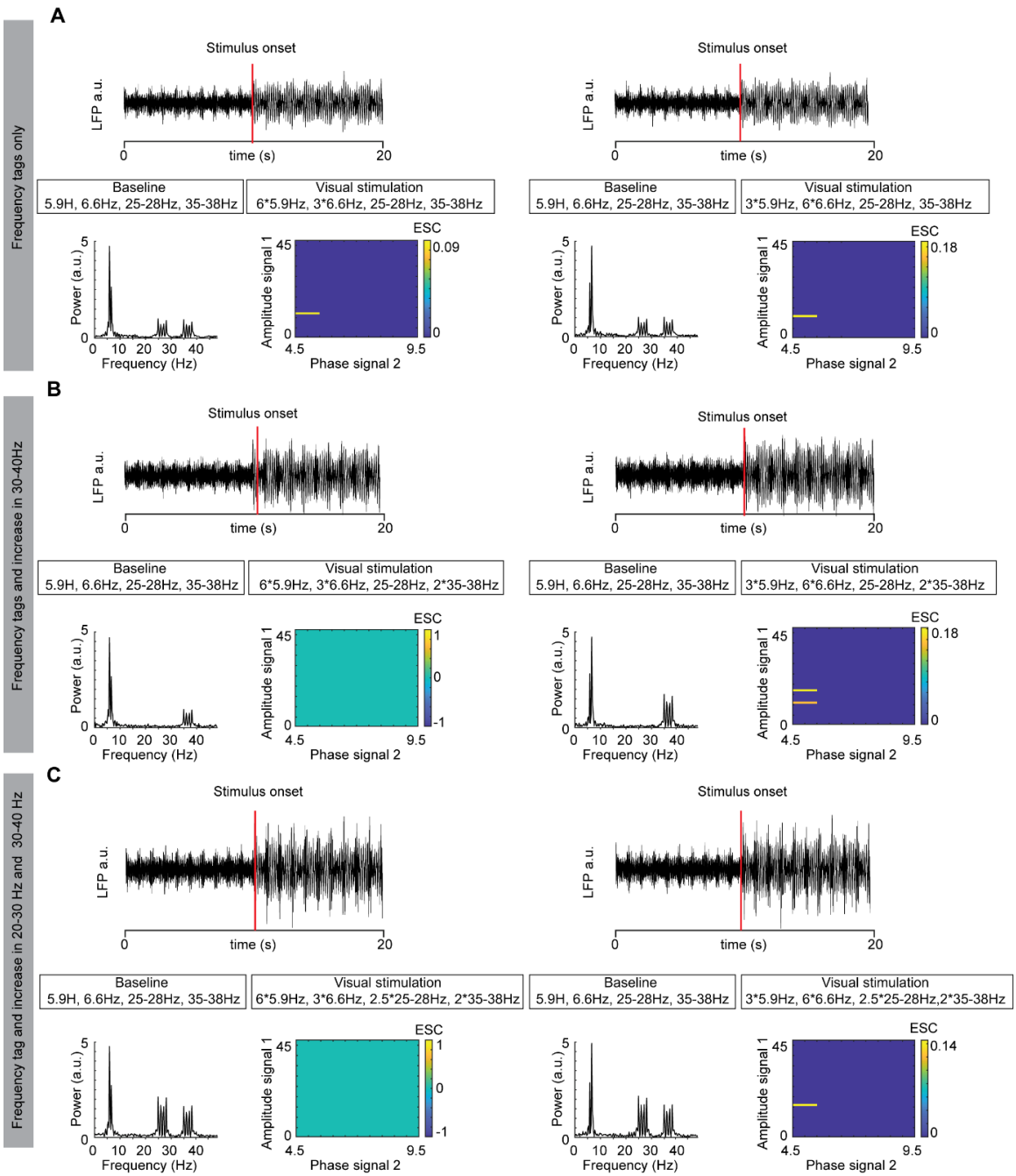

signal 1= 0-45 Hz endogenous frequencies
signal 2=4.5-9.5 Hz stimulation frequencies

Fig. S12. Simulation demonstrating that an increase in LFP amplitude alone does not promote increased correlation among simulated endogenous and evoked oscillations.

Data shows simulated local field potential (LFP) traces, generated by addition of sinusoidal signals of 5.9Hz, 6.6Hz, 25-28Hz and 35-38Hz as well as Gaussian white noise with a standard deviation of 2. Baseline data (pre stimulus onset) contained the same magnitude for all oscillation components. Post stimulus data varied in standard deviation (SD) from the other signals. Fast Fourier transformations of generated data revealed peak amplitudes at input oscillations

(Frequency spectra). For all simulations, envelope to signal correlation (ESC) analysis showed no significant correlations between amplitudes of endogenous frequencies (signal1) and the phase of the frequency tags (signal2), when phase was kept constant throughout the generated signals. A) Left: The amplitude of the two stimulation frequencies (frequency tags) was increased by 6 SD for 5.9Hz and 3 SD for 6.6Hz. Right: The amplitude of the two stimulation frequencies was increased by 3 SD for 5.9Hz and 6 SD for 6.6Hz. In both instances an increase in LFP amplitude did not alter the ESC between the phases of the stimulation frequencies (signal 2) and the amplitude of the endogenous frequencies (signal 1). B) We simulated an increase in the 35-38Hz frequency domain, which was observed during visual stimulation. For this purpose, additionally to an increase in stimulation frequencies as in A) we also increased 35-38Hz by 2 SD compared to baseline. No significant correlation was found between endogenous frequencies and the phase of stimulus frequencies. C) Last, we simulated an increase in the 35-40Hz and 25-28Hz frequency domains, in addition to our stimulation frequencies. Additional to the 2 SD increase in amplitude of the 35-38Hz oscillation compared to baseline we increased the 25-38Hz component by 2.5 SD. Again, we found no significant correlation between our endogenous frequencies and the phase of our stimulation frequencies.

SI References

1. R. Oostenveld, P. Fries, E. Maris, J.-M. Schoffelen, FieldTrip: Open Source Software for Advanced Analysis of MEG, EEG, and Invasive Electrophysiological Data. Computational Intelligence and Neuroscience 2011, e156869 (2011).
2. B. Rossion, K. Torfs, C. Jacques, J. Liu-Shuang, Fast periodic presentation of natural images reveals a robust face-selective electrophysiological response in the human brain. Journal of vision 15, 18 (2015).
3. A. Bruns, R. Eckhorn, Task-related coupling from high- to low-frequency signals among visual cortical areas in human subdural recordings. International Journal of Psychophysiology 51, 97–116 (2004).
4. A. C. E. Onslow, R. Bogacz, M. W. Jones, Quantifying phase–amplitude coupling in neuronal network oscillations. Progress in Biophysics and Molecular Biology 105, 49–57 (2011).
5. J.-P. Lachaux, E. Rodriguez, J. Martinerie, F. J. Varela, Measuring phase synchrony in brain signals. Human Brain Mapping 8, 194–208 (1999).
6. M. J. Grabowska, et al., Innate visual preferences and behavioral flexibility in Drosophila. Journal of Experimental Biology 221, jeb185918 (2018).
7. M. N. Van De Poll, E. L. Zajaczkowski, G. J. Taylor, M. V. Srinivasan, B. van Swinderen, Using an abstract geometry in virtual reality to explore choice behaviour: visual flicker preferences in honeybees. Journal of experimental biology 218, 3448–3460 (2015).
8. A. C. Paulk, L. Kirszenblat, Y. Zhou, B. van Swinderen, Closed-loop behavioral control increases coherence in the fly brain. The Journal of neuroscience 35, 10304–10315 (2015).
9. H. Bokil, P. Andrews, J. E. Kulkarni, S. Mehta, P. P. Mitra, Chronux: A platform for analyzing neural signals. Journal of neuroscience methods 192, 146–151 (2010).
10. , ggplot2 - Elegant Graphics for Data Analysis | Hadley Wickham | Springer (January 28, 2020).
11. D. Bates, M. Mächler, B. Bolker, S. Walker, Fitting Linear Mixed-Effects Models using lme4. arXiv:1406.5823 [stat] (2014) (January 28, 2020).
12. R. Nieuwenhuis, influence.ME: Tools for Detecting Influential Data in Mixed Effects Models. 4, 10 (2012).
13. , Pinheiro, J., Bates, D., DebRoy, S., Sarkar, D., & Team, R. C. (2012). nlme: Linear and nonlinear mixed effects models. R package version, 3(0). - Google Search (January 28, 2020).